PHILOSOPHICAL TRANSACTIONS OF THE ROYAL SOCIETY A MATHEMATICAL, PHYSICAL & ENGINEERING SCIENCES

Experimental Evaluation of the Deformation Path Concept

F. A. Donath and D. S. Wood

Phil. Trans. R. Soc. Lond. A 1976 **283**, 187-201
doi: 10.1098/rsta.1976.0078

Phil. Trans. R. Soc. Lond. A. **283**, 187–201 (1976) [187]
Printed in Great Britain

Experimental evaluation of the deformation path concept

By F. A. Donath and D. S. Wood
Department of Geology, University of Illinois, Urbana, Illinois, U.S.A.

[Plates 8 and 9 and colour plate I]

Study of natural finite strain states in several oolitic limestones indicates that, unlike most rocks, many limestones have undergone deformation by a process of approximately plane strain. Accordingly, specimens of oolitic limestone were deformed experimentally in plane strain at confining pressures of 100 and 200 MPa, at temperatures of 25, 100, and 200 °C, and to total strains from 20 to 50 % by increments of 10 and 5 %. From subsequent strain analysis, utilizing thin sections of the deformed specimens, we find that the greatest strain heterogeneity exists, as is to be expected, for conditions under which the rock has low ductility, i.e. low confining pressure and low temperature. Increased pressure and temperature promotes a change in microscopic mechanism from cataclasis to intracrystalline gliding. The degree of strain heterogeneity is significantly decreased at higher confining pressure; it is affected to a lesser degree by higher temperature. From our results, it appears that the degree of strain heterogeneity remains sufficient within the deformational mode fields of uniform flow and ductile faulting to justify utilization of the deformation path concept.

Introduction

Studies of deformed objects in rocks have often of necessity concentrated almost exclusively on aspects of geometry such as the orientation, symmetry, magnitude, and distribution of strain. More rarely, where circumstances permit, an attempt is made to ascertain the strain history of the rocks or of the structure in which the deformed objects are contained. The geometries of deformed objects tell nothing in and of themselves about the strain histories of the objects, of the rocks in which they occur, nor of the structures to which they are related. Thus, the deformation path concept is a very appealing and potentially useful one in structural geology. The concept was introduced by Flinn (1962) who described the manner in which an initial sphere is deformed progressively through a series of intermediate ellipsoidal shapes until the deformation is completed. The deformation path is the locus of the sequential intermediate ellipsoids which may be considered as the cumulative superposition of a finite number of incremental deformation ellipsoids. The simplest deformation paths result when the incremental deformation ellipsoids are of constant strain increment and the strain is irrotational. For ellipsoids with axes defined as $X > Y > Z$, such simple deformation paths are straight lines on the deformation plot, where X/Y is plotted as the ordinate and Z/Y is plotted as the abscissa in three special circumstances. These obtain where $X = Y > Z$, where $X > Y = Z$, and where $X/Y = Y/Z$ when Y has undergone no length change. In the general case, all other deformation paths will not define straight lines (Ramsay 1967, p. 329).

For a specific structure or region the data immediately obtainable usually consist only of the end points of many individual deformation paths which plot in a particular area, or field, of the deformation plot (Ramsay 1967, p. 141). No simple method exists for the derivation of a collective deformation path for the region or structure from the end points (of individual paths) which comprise the deformation field.

A good approximation for obtaining individual deformation paths by utilization of the normally heterogeneous small scale nature of finite strain was outlined by Wood (1974, p. 391). This method depends upon the fact that finite strain is heterogeneous on the scale of individual indicators (e.g. ooids) in a deformed rock (e.g. oolitic limestone) because of variable behaviour among the indicators and variation in frequency of indicators relative to matrix of slightly different ductility. A major assumption is involved – namely, that each fabric component experiences a similar strain history but, at any given time, different components may reflect different stages of that history. Thus, if all components underwent strain according to a single pattern but achieved different magnitudes of finite strain, they would statistically lie on an individual deformation path. If this were the case, those components with the highest strain value would, during their deformational history, have passed through the stages represented by objects with lower strain values.

Clearly, successful application of this approach requires (1) that the principal assumption as stated above, be true, and (2) that a sufficient degree of strain heterogeneity exist, such that a continuous deformation path can be established. As the homogeneity of deformation increases, the deformation path, as reflected in the deformed components, may become discontinuous and possibly ambiguous.

Considering the appeal and usefulness of the deformation path concept in its application to naturally deformed sequences, we felt that the concept should be evaluated systematically under controlled experimental conditions. The decision to undertake such an experimental evaluation having been made, it was then necessary to select an appropriate material, a representative type of strain, and realistic environmental conditions for the study.

Ideally, one would like to have rock specimens comprised of closely packed spherical objects which would deform by one or another of several possible deformation mechanisms depending upon the conditions imposed. Oolitic limestone seems to meet these requirements best in that (1) it includes spherical objects having similar properties and behaviour as the enclosing cement, and (2) calcite deforms by a variety of fracture and frictional mechanisms (cataclasis) and intracrystalline gliding mechanisms under different conditions of deformation readily controlled in the laboratory. The type of strain to which the rock was to be subjected was determined after consideration of the finite strain observed in naturally deformed limestones, discussed below, and the selected conditions of pressure (up to 200 MPa) and temperature (up to 200 °C) were felt to be realistic for natural deformation at depths in the Earth's crust up to 8 km. The selected strain rate (10^{-4}/s) was necessarily less realistic. This was not considered to be a serious limitation, however, inasmuch as concern was with the degree and distribution of strain heterogeneity as a function of the total strain and operative deformation mechanisms. The rock was deformed dry, no recrystallization flow was observed, and our conclusions therefore apply strictly to deformation by cataclastic and intracrystalline gliding flow. For cataclastic flow, the deformation is not affected by strain rate (Donath & Fruth 1971).

The study reported here was carried out with specially modified triaxial deformation apparatus and consists of two series, one run at 100 MPa and the second at 200 MPa. Both series included tests run at 25, 100, and 200 °C to total strains from 20 to 50 % by increments of 10 %, and occasionally 5 %. Most tests were repeated to check reproducibility. With duplications, a total of 61 tests were run. Cylindrical specimens, 12 mm diameter by 32 mm length, were used. Thin sections were obtained from most specimens and were utilized for detailed strain analysis.

Natural finite strain in limestones

The most convenient means of representing finite strain states is afforded by the deformation plot (Flinn 1956, 1962) on which deformation ellipsoids with all possible axial ratios can be plotted. Particularly useful is the logarithmic deformation plot (Wood 1974, Fig. 1) which has the advantage that similar values of dimensional change in each of the three principal directions (X, Y, Z) compared to the equivalent volume sphere diameter (d) are straight lines. Deformation induced in a test specimen shortened by standard triaxial compression would ideally produce oblate spheroids that would plot along the abscissa; deformation induced in a test specimen elongated in a standard triaxial extension test would be expected to produce prolate spheroids that would plot along the ordinate. With increased shortening or elongation, and, hence, increasing departure from the spherical, these spheroids would plot progressively further along their respective axes.

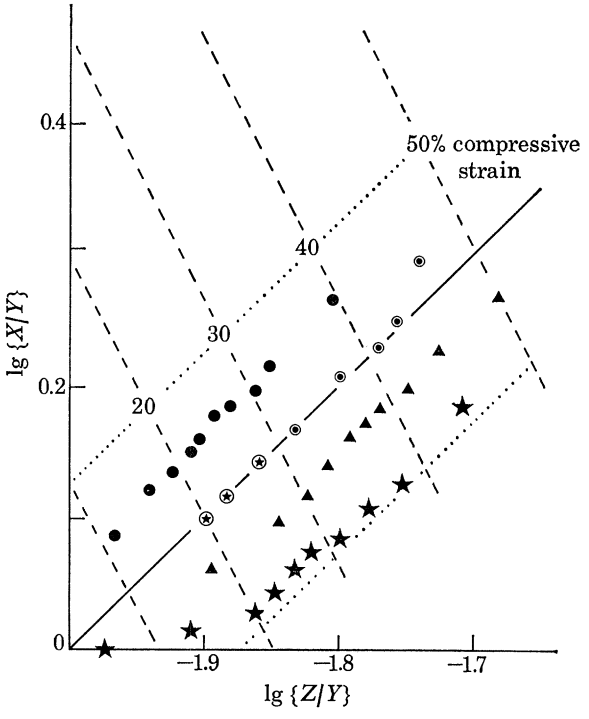

Figure 1. Logarithmic deformation plot with deformation paths for five naturally deformed limestones. ●, Hirnant limestone (U. Ordovician, Cwm Hirnant, Wales); ⊛, Carboniferous limestone (Baltic Quarry, near Merthyr Tydfil, Wales); ⊙, Conococheage limestone (U. Cambrian, Hagerstown, Md., U.S.A.); ▲, Carboniferous limestone (Morlais Quarry, Dowlais, Wales); ★, Islay limestone (L. Dalradian, Loch Allallaidh, Islay, Scotland). Line of unit slope through origin indicates plane strain, i.e. no dimensional change in the Y direction.

Finite strain data from five naturally deformed limestones from Wales, Scotland, and the United States are plotted on the logarithmic deformation plot in figure 1. The deformation paths are based upon a large number of measurements of ooid ratios made in each of the three symmetry planes of the deformation ellipsoid. The individual measurements in each plane have been sorted into order of increasing departure from circular, and then associated as complete axial ratios according to the method outlined by Wood (1974) which makes the assumption

that the most deformed objects seen in one symmetry plane should be associated with the most deformed objects seen in another symmetry plane. These derived ellipsoids are typically obtained for either 10 or 20 % samples of the total range of strain values. Plotting of the mean value of each such sample gives the distribution of points (figure 1) which constitutes an *individual* deformation path for a given locality. The data from the Baltic Quarry, near Merthyr Tydfil, Wales, represent a special case in that they are the mean states of strain determined for three adjacent zones approaching a small thrust fault. In this instance, it is valid to assume that the manner of deformation would have been similar in each of the zones and that this deformation path, therefore, is a close approximation to a purely natural *collective* deformation path.

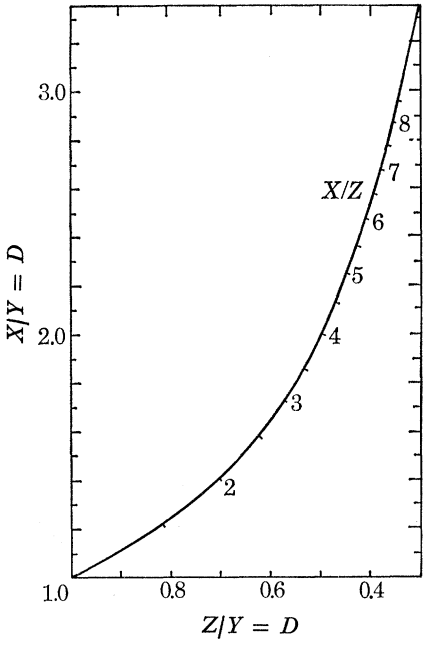

FIGURE 2. Arithmetic deformation plot. Curve indicates plane strain.

The dashed lines in figure 1 indicate the percentage shortening in the Z direction (compressive strain); the dotted lines indicate ± 10 % shortening in the Y direction. It is noteworthy that, although all five rocks have been shortened in the Z direction 30–50 %, none shows a change in the Y direction greater than 10 %, i.e. all tend to approximate very closely a state of plane strain. Perfect plane strain, in which no dimensional change occurs in the Y direction, would be represented in figure 1 by points that plot along the line of unit slope through the origin. In the arithmetic plot of figure 2, points representing plane strain would plot along the curve.

The data of figure 1 suggest that naturally deformed limestones may characteristically deform in a manner closely approximating plane strain. For deformation by plane strain, the strain in the X and Z directions can be determined quite easily from the X/Z ratio by utilizing a deformation plot like that of figure 2. Measurement of the longest (X) and shortest (Z) axes in a section cut perpendicular to Y yields individual X/Z ratios that can be located along the plane strain curve. Projection of these points (ratios) onto the respective coordinate axes gives the X/Y and Z/Y ratios which, because Y is unchanged from the initial diameter of the equivalent volume sphere, are the strains in the X and Z directions, respectively. The analysis of strain

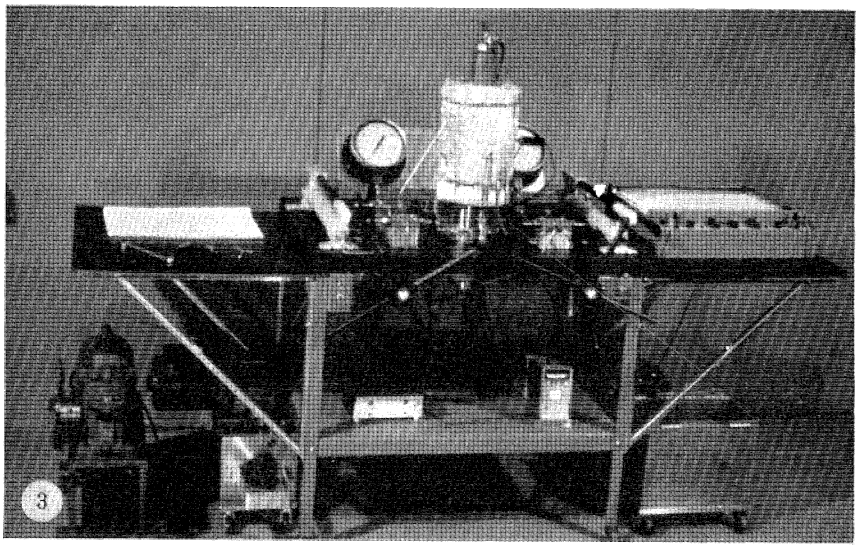

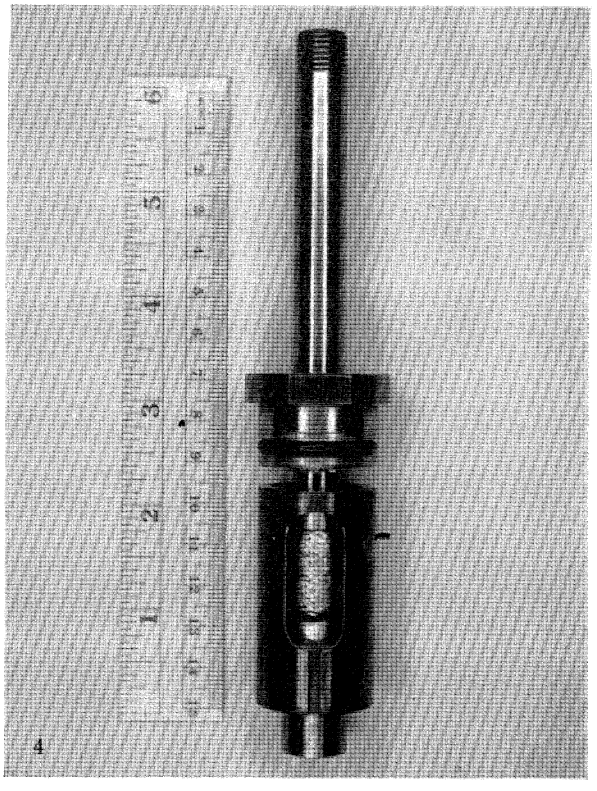

FIGURE 3. Triaxial deformation apparatus. Pressure vessel is shown with heating jacket in place for high temperature experiment. Axial loading pump is positioned beneath bench extension.

FIGURE 4. Constrictor used to effect plane strain condition. Piston-specimen-anvil assembly is shown positioned within constrictor. Specimen has been subjected to 30% shortening.

(*Facing p.* 191)

PHILOSOPHICAL TRANSACTIONS OF THE ROYAL SOCIETY A MATHEMATICAL, PHYSICAL & ENGINEERING SCIENCES

in deformed limestone therefore is much simplified and requires detailed measurement in only one, rather than in three planes. Data thus obtained are plotted directly along the plane strain curve of whichever plot (arithmetic or logarithmic) is used.

Methods of study

Apparatus

The testing apparatus is shown in figure 3. As indicated above, standard triaxial compression testing would be expected to produce oblate spheroids that would plot along the abscissa of the deformation plot. A modification of standard apparatus was therefore necessary if plane strain, consistent with that determined for natural deformation of limestones, was to be achieved experimentally. This was accomplished by inserting the piston–specimen assembly into a specially designed constrictor (figure 4), which, in turn, fits inside the triaxial pressure cell. The parallel internal faces of the constrictor make tangential contact with the jacketed cylindrical specimen along its diameter and prevent the specimen diameter from expanding perpendicular to these faces. Thus, a plane strain condition is approximated in the plane parallel to the internal faces of the constrictor. Constraint perpendicular to these faces causes the stress to increase in this direction (Y) and to become a true intermediate principal stress. This has two effects in addition to inducing plane strain in the specimen: first, the mean stress is increased and the rock becomes stronger (see figure 7); and, second, the strikes of any faults produced in the deformed specimens are oriented perpendicular to the faces of the constrictor.

Testing procedure

Because of the large (for experimental deformation) axial strains desired for certain specimens in this study, special procedures had to be developed to minimize apparatus effects on the modes and homogeneity of deformation – indeed, even to achieve the total strains desired. Standard specimen size is typically 12 mm diameter by 25 mm length. It was found that significant bulging of the specimen and 'intrusion' of the piston and anvil into the ends of the bulged specimen had occurred by 30 % axial strain for standard-length specimens when deformed in the constrictor. Further deformation only reflected these boundary conditions and was thus an artifact of the testing procedure. Specimens 32 mm long were therefore utilized and not deformed beyond 30 % axial strain initially. Negligible bulging was observed for these specimens. To achieve larger axial strain, the specimens were removed from the test apparatus and were reground to cylindrical form. These were then rejacketed, again placed in the constrictor, and deformed up to an additional 20 % axial strain. The length of the specimen was not affected by the regrinding process.

Figure 5 shows representative load–displacement curves for tests run at room temperature and 100 and 200 MPa confining pressure. The two stages of deformation are reflected in the unloading and reloading portions of the respective curves at about 30 % shortening. Regrinding of the specimen results in a reduced cross-sectional area over which the axial load is applied; hence, in the second stage of deformation, less axial force is required to produce the equivalent axial stress of the preceding stage. The second stage curves must be visually shifted upward to appreciate the continuity of the load–displacement plot. Corrections for area change in calculating the differential stress automatically remove the apparent discontinuity from the stress–strain curves (figure 7). It is noteworthy, also, that the rock shows development of a significant

yield stress in the second stage deformation – that is, a significant differential load must be applied before further shortening occurs, in marked contrast to its behaviour in the first stage deformation.

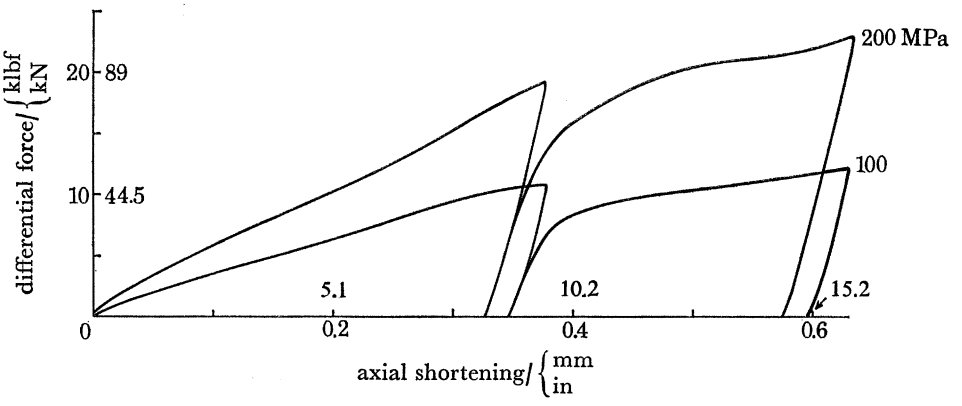

FIGURE 5. Load-displacement curves for Inferior oolite deformed at 25 °C, 100 and 200 MPa. Specimen has been deformed 30 % in first stage, removed from pressure vessel, reground, and deformed an additional 20 % in second stage (*see* text).

Material used

The rock selected for study is the Inferior oolite (Jurassic; Chipping Camden, Oxfordshire, England) which is believed to have been subjected to a depth of burial no greater than 500 m. The block of Inferior oolite from which test samples were taken has a porosity of 23.9 ± 0.4 % and shows no evidence of mechanical twinning. That this rock has been subjected to a relatively simple burial history and has retained its deformational virginity can perhaps best be appreciated by comparing its deformational properties with that of a typical undeformed oolitic limestone which has been subjected to deeper burial and has been buried for a much longer period of time. The Crown Point limestone (Ordovician; Plattsburg, New York, U.S.A.) has been selected for comparison; it has a porosity of 0.5 ± 0.1 % and has been subjected to a depth of burial possibly as great as 3000 m. Approximately 16 percent of the calcite grains and ooids contain twin lamellae.

Figure 6 shows curves of differential stress versus axial strain for the Inferior oolite and for the Crown Point limestone deformed in standard triaxial compression tests at 25 °C and 100 MPa confining pressure. Under these conditions the Crown Point limestone has a yield stress and an ultimate strength both in excess of 350 MPa at an axial strain of about 2 %. Under identical conditions the Inferior oolite is extremely weak, has no definable yield stress, and deforms continuously with increasing differential stress until it reaches an ultimate strength of about 230 MPa beyond 25 % axial strain. The Inferior oolite appears to be appropriately named in terms of its mechanical properties as well as its stratigraphic position!

At room temperature, the Inferior oolite undergoes a porosity loss of 9.6 % when subjected to 100 MPa hydrostatic pressure. An additional 8.4 % loss occurs as a consequence of applying differential stress and deforming the rock to 30 % axial strain. The application of 200 MPa hydrostatic pressure causes a 15.6 % reduction in porosity. Applied differential stress and induced axial strain of 30 % results in an additional 8.3 % porosity reduction – that is, the original porosity is lost entirely by 30 % strain at the higher pressure.

Strain analysis

Thin sections of deformed test specimens of Inferior oolite were cut parallel to the plane-parallel faces of the constrictor, i.e. perpendicular to Y. Thus, the longest and shortest axes of the deformed ooids lie in the section and permit ready determination of X/Z ratios. In addition, the strike of intergranular fractures, faults, and shear zones is perpendicular to the section, and the characteristics and geometry of these features can therefore be studied in cross section with respect to the directions of the extreme principal stresses.

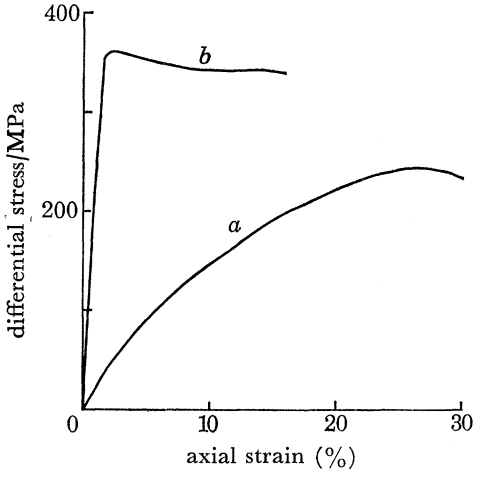

FIGURE 6. Curves of differential stress against axial strain for (*a*) Inferior oolite and (*b*) Crown Point limestone; 100 MPa, 25 °C.

The distribution of X/Z ratios and the derived principal strains were studied in two ways. First, the total population of ratios for a given section (representing a given set of test conditions) was subdivided into five equal parts, representing 20% samples of increasing departure from circular. The mean ratios for each part were determined, and these five means were used to define a deformation path. The deformation paths thus derived can be compared with one another both to evaluate the basic premise of the deformation path concept, as given in the Introduction, and to evaluate the effects of different test parameters. Second, the spatial distribution of the strains can be studied to determine the degree of homogeneity and its relationship to the different test parameters. Both approaches were applied and are discussed below.

DEFORMATIONAL BEHAVIOUR OF INFERIOR OOLITE

The deformational behaviour of rock can be conveniently discussed in terms of the physical resistance to applied differential stress, or stress–strain relationships, and the macroscopic expression of the processes of deformation, or deformational modes (Donath *et al.* 1971). Both are highly dependent on the rock type, on the environmental conditions of deformation, and on boundary conditions. Although calcite and various limestones have been much studied in experimental rock deformation, and the environmental conditions (pressure, temperature, strain rate) used in this study are not unusual, the boundary conditions imposed and the mechanically virgin nature of the rock are unusual in this instance. As a consequence, the Inferior oolite shows both anticipated and unexpected behaviour.

PHILOSOPHICAL TRANSACTIONS OF THE ROYAL SOCIETY A MATHEMATICAL, PHYSICAL & ENGINEERING SCIENCES

Stress–strain relationships

Curves of differential stress versus axial strain for the Inferior oolite are given in figure 7 for both test series, 100 MPa (1000 bar) and 200 MPa (2000 bar), at the three temperatures considered, 25, 100 and 200 °C. It should be noted that each curve in figure 7, with the exception of that for the triaxial test, actually is comprised of a minimum of four curves – one for a test terminated at 20 % axial strain, a second for termination at 30 %, a third at 40 %, a fourth at 50 %, plus curves for tests at intermediate strains and for repeated tests. For the 24 principal combinations of test conditions considered in this study, the reproducibility typically was better than ± 1.5 %; in only one instance did it exceed ± 2.5 %. Although the relationships among the curves shown in figure 7 are certainly indicative and probably accurate, differentiation among those in each pressure series can be made with confidence only at strains larger than 30 %, in spite of the excellent reproducibility. The remarks made below should be considered with this qualification in mind.

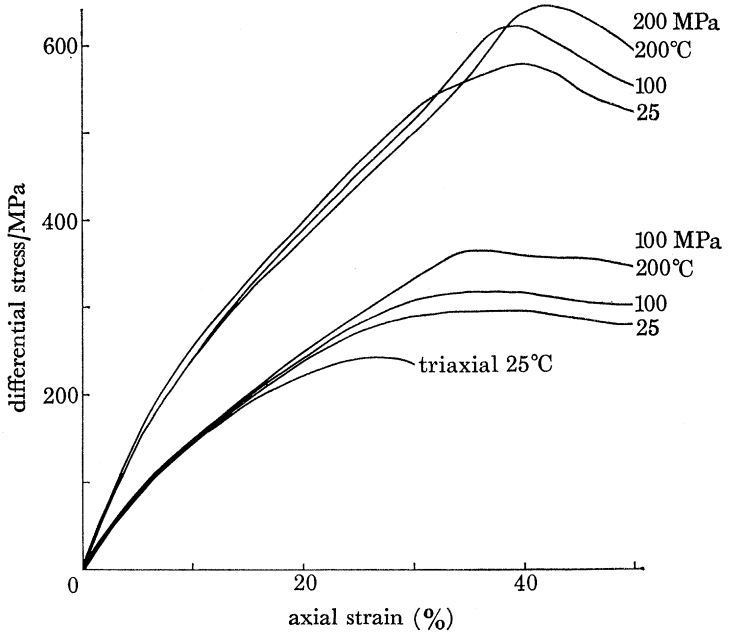

FIGURE 7. Curves of differential stress against axial strain for Inferior oolite, deformed with constrictor: 100 and 200 MPa; 25, 100, and 200 °C.

An immediately obvious effect which might be pointed out first is that of the constrictor on the strength of the oolite. A curve for a standard triaxial compression test at 25 °C and 100 MPa is given in figure 7 to permit comparison for the same environmental conditions with and without the constrictor. As mentioned above, the presence of the constrictor results in an increased intermediate principal stress and, hence, increased mean pressure; the strength of the oolite is consequently increased. It appears that for these conditions the ductility is also enhanced; fracturing has been suppressed by the higher mean pressure and by the physical constraint of the constrictor, and deformation has proceeded to 50 % total strain without loss of cohesion for the specimen as a whole. (It should be mentioned that at 200 °C and 200 MPa, however, a total strain of more than about 48 % could not be achieved without violent fracture.)

The specimen subjected to standard triaxial compression would have suffered a total loss of cohesion within a few percent beyond 30 % axial strain if the test had been continued.

A second observation of interest is the absence of any well defined yield stress. Unlike other limestones which require moderate to high differential stress before deforming more than 1 or 2 %, the Inferior oolite appears to yield continuously almost immediately after the application of differential stress (figure 6). The closest analogy of which we are aware is the obliteration of the yield stress in transverse cores taken from previously strained parent cores of limestone (Donath 1970). This behaviour in the Inferior oolite is presumed to reflect two factors: the high initial porosity, and the completely random orientation of calcite grains which provides numerous grains favourably oriented for *e* twinning, a mechanism activated at very low stress levels. In addition to the cataclastic deformation promoted by the high porosity and consequent local stress concentrations, these concentrations would also likely induce twinning (and possibly translation gliding) in adjacent, less favourably oriented grains (cf. Friedman 1963).

Undoubtedly the most unexpected observation regarding the mechanical properties of the oolite is that, at both confining pressures, the rock is weakest at room temperature and strongest at 200 °C at axial strains greater than about 35 %. This is in marked contrast with the observed decrease in strength with increased temperature normally found for limestones (e.g. Handin & Hager 1958). The difference appears to be related to the relative contributions of cataclasis and intracrystalline gliding to the deformation and to the related development of shear zones, i.e. ductile faults.

The differential stress sustained by the oolite continues to increase with increasing strain as long as the deformation is uniformly distributed throughout the specimen, i.e. as long as the macroscopic deformation is reasonably homogeneous. However, when the deformation, especially cataclasis, begins to become concentrated in zones, the rock begins to lose some resistance to the applied differential stress. From this point on, whether the rock shows a lower positive slope in the stress–strain curve, maintains a reasonably constant differential stress, or shows a negative slope depends principally upon the relative contributions of cataclasis and intracrystalline gliding and on the characteristics of the developing shear zone(s). The shear zones developed in the Inferior oolite typically result in the macroscopic mode of deformation called a ductile fault (see Donath *et al.* 1971) and do not result in loss of cohesion for the specimen as a whole (except at strains greater than 48 % at 200 °C and 200 MPa.) The approximate strains at which ductile faulting is initiated are plotted in figure 8 as a function of temperature for each pressure series. Because the percentage strain before faulting can be taken as a measure of ductility, this also represents the effect of temperature on ductility in the oolite.

It is clear that increased temperature retards the development of shear zones (cf. figure 8), but it is not clear whether temperature also effects a real separation of the stress–strain curves before shear zone initiation (cf. figure 7). This latter possibility presents more of a problem at the lower rather than at the higher pressure. At the higher pressure (200 MPa) the separation, however slight, is consistent with the generally accepted observation that increased temperature lowers strength. Because most of the initial porosity is lost when the hydrostatic pressure is applied, thus affecting the extent and nature of cataclasis, and because the magnitude of differential stress required at that pressure is sufficient to activate *r* translation gliding in the calcite, which is temperature dependent, the apparent temperature effects on strength at that pressure up to axial strains of 30 % can be readily explained. The high pressure, which greatly

PHILOSOPHICAL TRANSACTIONS OF THE ROYAL SOCIETY A MATHEMATICAL, PHYSICAL & ENGINEERING SCIENCES

reduces porosity and creates high normal stress and greater frictional resistance that inhibits cataclastic processes, and the activation of an additional significant slip system act together to promote homogeneous macroscopic strain and normal (i.e., expected) behaviour. At sufficiently high strains, however, cataclasis becomes relatively more important and results in the development of shear zones that, beyond 30 % strain, lead to yielding, an ultimate strength, and subsequent loss of resistance to differential stress. Because the shear zones are initiated at smaller strains at the lower temperatures, the rock shows lower strengths at the lower temperatures.

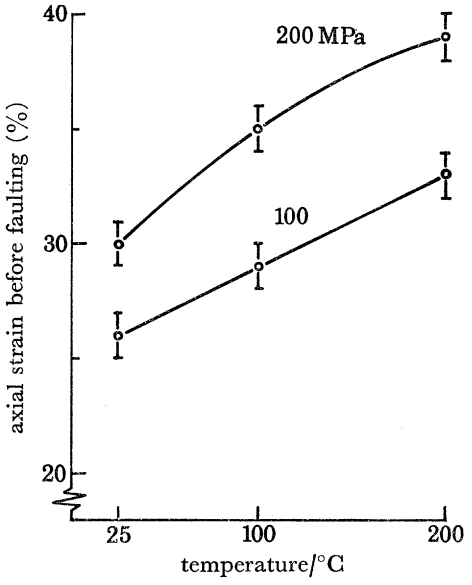

FIGURE 8. Axial strain before faulting (ductility) against temperature, Inferior oolite.

For the results at 100 MPa confining pressure, the apparent greater strength below 30 % strain of the oolite deformed at the higher temperatures may, if real, reflect a greater homogeneity of deformation induced by higher temperature. Because at this pressure and at room temperature the oolite still retains much of its initial porosity after the application of hydrostatic pressure, cataclasis can be expected to be significant even though *e* twinning will occur readily at the stress levels developed during deformation. Porosity reduction under hydrostatic pressure may be greater at higher temperatures, thus possibly affecting the amount or distribution of cataclasis during subsequent deformation, or the higher temperature may influence in some other way the homogeneity of deformation. It is apparent, however, that the shear zones develop at larger strains at higher temperatures and, hence, at higher differential stress at higher temperatures. Clearly, once the shear zones become established, the sustained differential stress beyond this point reflects their presence. In general, any factor that affects the degree of cataclasis will affect the subsequent deformational behaviour of the rock.

Deformational modes

As indicated by the data of figure 8, the Inferior oolite is a very ductile rock under the conditions of this study. Even at the lower pressure and at room temperature the rock must deform approximately 25 % before individual ductile faults begin to develop; another several percent strain is required to produce recognizable shear zones under these conditions. Still larger strains

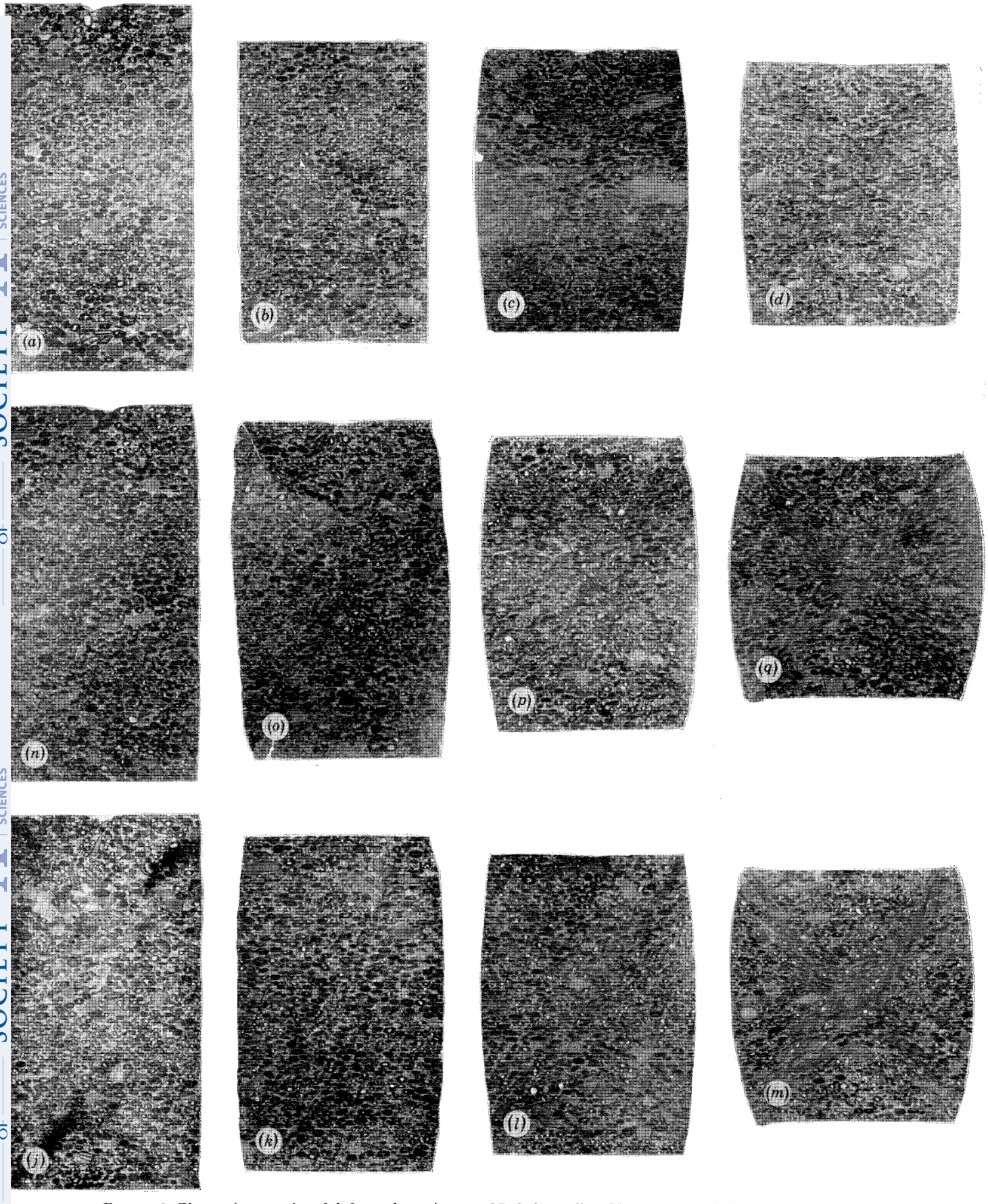

FIGURE 9. Photomicrographs of deformed specimens of Inferior oolite. Top row: 200 MPa, 200 °C: *a*, 20 %, *b*, 30 %; *c*, 40 %; *d*, 45 % strain. Middle row: 100 MPa, 200 °C: *n*, 20 %; *o*, 30 %; *p*, 40 %; *q*, 50 % strain. Bottom row: 200 MPa, 25 °C: *j*, 20 %; *k*, 30 %; *l*, 40 %; *m*, 50 % strain.

(*Facing p.* 196)

PHILOSOPHICAL TRANSACTIONS OF THE ROYAL SOCIETY A MATHEMATICAL, PHYSICAL & ENGINEERING SCIENCES

are required to produce shear zones at higher pressure and higher temperatures. The deformation observed in this study thus moves with increasing strain from the deformational mode field of uniform flow to that of ductile faulting (see Donath *et al.* 1971), and the modes of deformation observed are, therefore, uniform flow and ductile faulting.

Photomicrographs of thin sections of the deformed Inferior oolite are shown in figure 9. Three sequences are presented to illustrate the effect of increasing strain on the mode, and homogeneity, of deformation at different confining pressures and temperatures. Although the shear zones (ductile faults) present at 50 % strain at both 100 MPa–200 °C and 200 MPa–25 °C are obvious, the point (percent strain) of their initiation earlier in the sequence may not be apparent from casual observation; indeed, careful thin section examination is required. Initiation under the former set of conditions occurs shortly after the stage represented by the second thin section (*o*) in the sequence; under the latter set of conditions, individual ductile faults are just beginning to appear at the stage represented by the second thin section (*k*). At 200 MPa–200 °C, individual ductile faults begin to develop shortly before the stage represented by the third thin section (*c*) in the sequence. Although well developed shear *zones* are not present in the fourth section of this sequence (*d*), in contrast to the other two sequences, well defined individual ductile faults are present.

Interestingly, the width of shear zones is affected differently by temperature and pressure. Increased confining pressure at low temperature typically causes the zones to become broader, whereas increased temperature causes the shear zones to become narrower until, in some instances, a zone becomes a single surface of ductile faulting (see Olsson 1974). This is the situation in the Inferior oolite at 200 MPa and 200 °C. As mentioned above, at these conditions ductile faulting gives way to violent fracture (brittle faulting) at strains larger than about 48 %.

The degree of homogeneity of deformation can be appreciated in a qualitative manner from a consideration of the deformational modes. Macroscopic homogeneity obviously decreases with increasing development of shear zones and, hence, with increasing total strain. Homogeneity increases with higher confining pressure and higher temperature. The homogeneity of deformation will be considered on a quantitative basis in the next section.

Strain distribution

Strain homogeneity

The long (X) and short (Z) axes of the elliptical cross-sections of 150–250 ooids were measured in each thin section of a deformed specimen selected for study. The ooids were randomly chosen throughout a section and provided a distribution of X/Z ratios which permitted individual X and Z strains to be determined from place to place throughout the X/Z plane of the specimen. As discussed above, this was made possible by the existing plane strain condition. The strain values thus obtained were contoured to determine the variation of strain within the X/Z plane of the specimen. Because this plane is perpendicular to the strike of any faults present, any variation related to faults or to shear zones would also be readily apparent.

The twelve contour diagrams showing strain in the Z (axial or compression) direction for the test series at 200 MPa confining pressure are given in figure 10. The compressional strain is contoured at 5 % intervals. In comparing these results with the total strain indicated for a given section, or with the stress–strain curves of figure 7, one should note that the strains indicated in figure 10 (and also in figure 11) reflect the strain of individual components in the rock. The axial

strain indicated in figure 7, and for individual specimens, is the bulk strain referred to the original length of the specimen. Because the application of confining pressure causes axial strain of about 3.3 and 5.5 % at pressures of 100 and 200 MPa, respectively, through the reduction of porosity, the bulk strains will exceed the average component strains by approximately these amounts.

Comparison of the contour diagrams for the 200 MPa–200 °C tests (figure 10) with the corresponding thin sections (figure 9) provides some interesting insights into the nature of the deformation. Although the development of ductile faulting is somewhat obscure in the sections, the concentration of relatively high compressional strain within conjugate zones is quite obvious in the strain contour diagrams. Thus, although the ductile faults in this instance may be sharply defined individual surfaces, clearly the grains in the immediate vicinity of these faults are being subjected to rather high, localized strain. Similarly, the development of shear zones (ductile faults) in the sequences at 100 °C and at 25 °C are clearly seen in the distribution of compressional strain in these specimens.

Possibly of even greater usefulness, the strain contour diagrams illustrate very clearly the effect of temperature on the homogeneity of deformation. For example, compare figure 10*k* with *f* and *b*, all of which show the strain distributions in specimens deformed at 200 MPa confining pressure to total strains of 30 %. Higher temperature clearly results in more homogeneous deformation of the oolite. Specimens deformed to 20 % (figures 10*j*, *e*, *a*), 40 % (figures 10*l*, *g*, *c*), and 50 % (figures 10*m*, *h*, *d*) also show this effect quite clearly and, in the last instance, even dramatically.

Examination of the strain contour diagrams of figure 10 indicates that for the conditions of this study, especially for the specific boundary conditions imposed, a possibly far more serious concern than ambiguity of a deformation path caused by deformation that is too homogeneous, is the possibility that the presence of incipient as well as fully developed shear zones may prevent the determination of a meaningful deformation path. This question will be addressed in the next section.

Deformation paths

The populations of X/Z ratios were utilized, as described above, to obtain the mean X/Z ratios for each of five (20 %) data samples for each section analysed. These were used to obtain the strains in the X and Z directions, respectively. The results for the data at 200 MPa are given in table 1 and are plotted on the logarithmic deformation plot of figure 11. Each set of symbols (i.e. circles, triangles, squares, stars) represents a possible deformation path for an individual experiment. Increased homogeneity of deformation would reduce the range of strains produced and, hence, the length or 'spread' of individual paths. At the extreme, perfect homogeneity would result in a single point. It will be noted that the increased homogeneity with increased temperature, recognized from the strain contour diagrams, is clearly reflected in a decreased spread of the individual paths. Compare, the example, the spread of data for the 50 % specimen (stars) at 25 °C with that for the 50 % specimen at 200 °C, or the 20 % data (circles) at these temperatures.

Description of plate I

Figure 10. Strain contour diagrams for specimens of Inferior oolite, 200 MPa. Top row: 200 °C; left to right; *a*, 20 %; *b*, 30 %; *c*, 40 %; *d*, 45 % strain. Middle row: 100 °C: left to right; *e*, 20 %; *f*, 30 %; *g*, 40 %; *h*, 48 % strain. Bottom row: 25 °C; left to right; *j*, 20 %; *k*, 30 %; *l*, 40 %; *m*, 50 % strain.

PHILOSOPHICAL TRANSACTIONS OF THE ROYAL SOCIETY A MATHEMATICAL, PHYSICAL & ENGINEERING SCIENCES

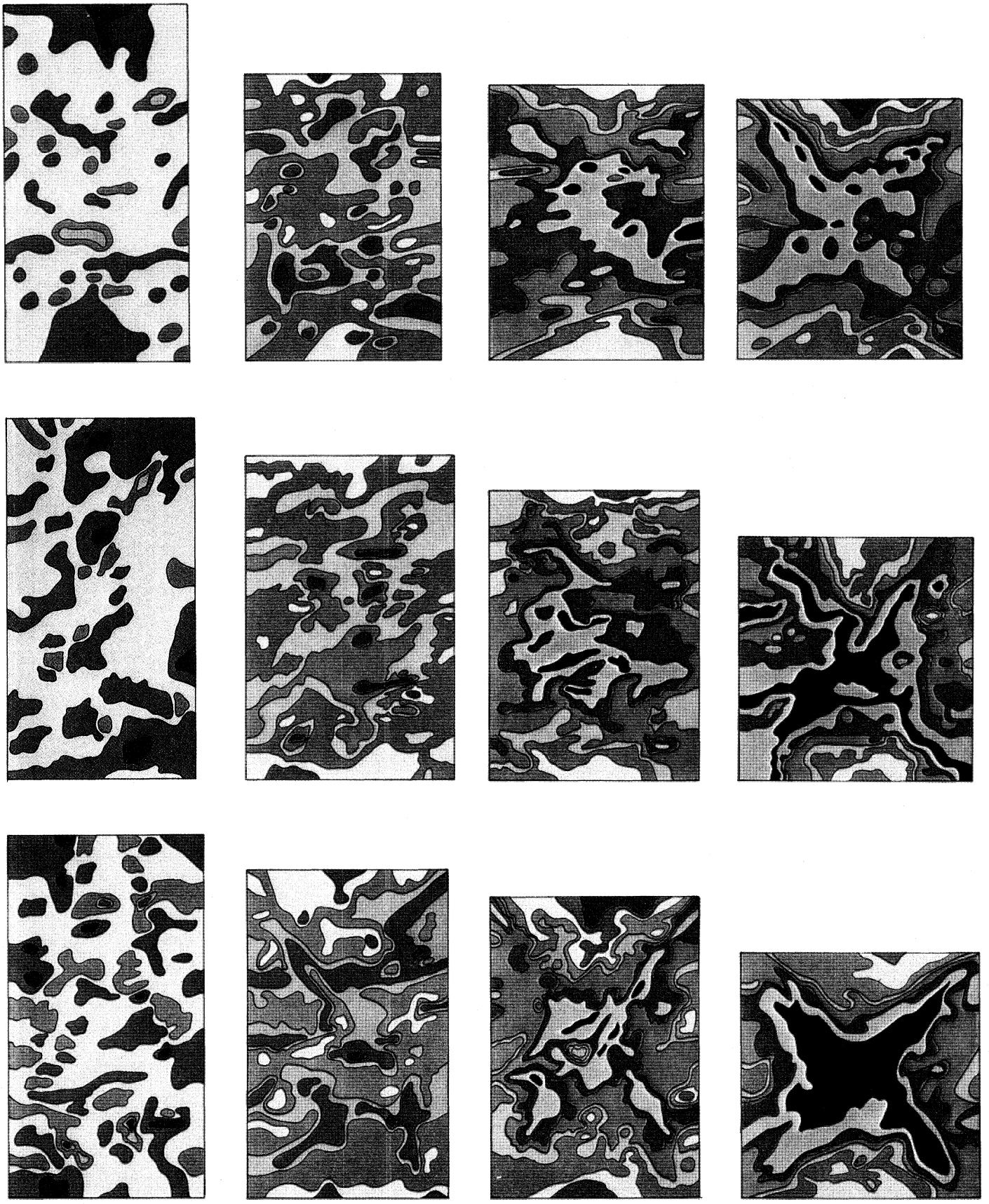

FIGURE 10. For description see opposite.

PHILOSOPHICAL TRANSACTIONS OF THE ROYAL SOCIETY A MATHEMATICAL, PHYSICAL & ENGINEERING SCIENCES

TABLE 1. OOID AXIAL RATIOS FOR SPECIMENS DEFORMED AT 200 MPa

temp. °C	total strain 20 %	30 %	40 %	50 %
200	1.14–1–0.88	1.25–1–0.80	1.31–1–0.76	1.33–1–0.75
	1.18–1–0.85	1.31–1–0.76	1.47–1–0.67	1.49–1–0.67
	1.21–1–0.83	1.35–1–0.73	1.57–1–0.63	1.58–1–0.63
	1.23–1–0.81	1.40–1–0.71	1.66–1–0.59	1.68–1–0.59
	1.30–1–0.76	1.50–1–0.66	1.83–1–0.54	1.79–1–0.55
100	1.12–1–0.89	1.21–1–0.82	1.28–1–0.78	1.31–1–0.76
	1.17–1–0.86	1.28–1–0.77	1.40–1–0.71	1.47–1–0.67
	1.20–1–0.84	1.37–1–0.74	1.50–1–0.66	1.60–1–0.62
	1.22–1–0.82	1.40–1–0.71	1.57–1–0.62	1.74–1–0.57
	1.28–1–0.78	1.52–1–0.65	1.76–1–0.57	2.00–1–0.50
25	1.12–1–0.89	1.22–1–0.82	1.24–1–0.80	1.28–1–0.77
	1.18–1–0.86	1.28–1–0.78	1.38–1–0.73	1.41–1–0.70
	1.21–1–0.84	1.31–1–0.76	1.47–1–0.67	1.60–1–0.62
	1.23–1–0.82	1.37–1–0.73	1.57–1–0.63	1.74–1–0.57
	1.32–1–0.75	1.42–1–0.70	1.77–1–0.56	2.12–1–0.47

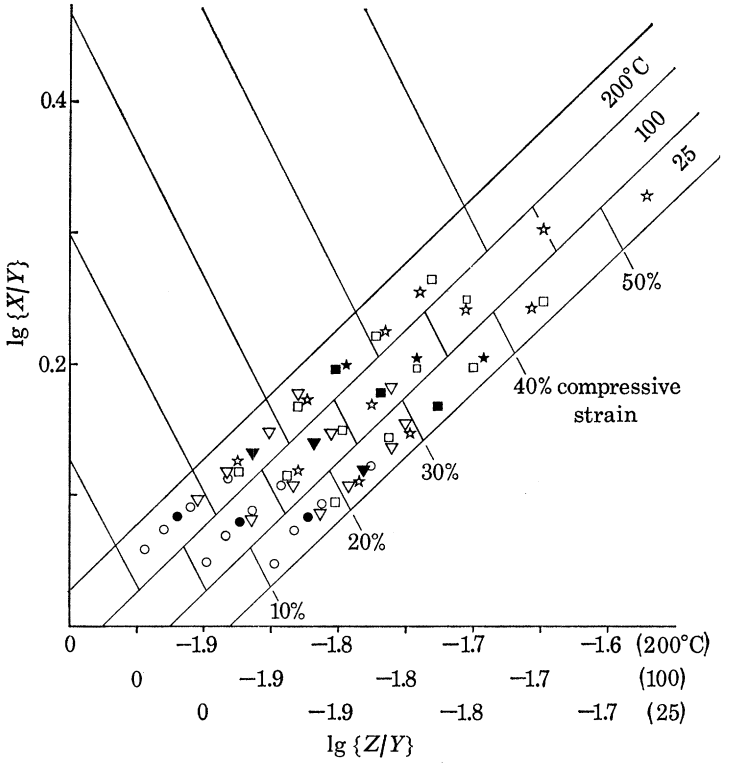

FIGURE 11. Logarithmic deformation plot for experimentally deformed Inferior oolite: 200 MPa; 25, 100 and 200 °C. Means of subgroup data for each specimen indicated by respective symbols: for specimens deformed 20 % (circles), 30 % (triangles), 40 % (squares), and 50 % (stars). Filled symbols indicate central mean of total population for each specimen. The percent compressive strain reference lines for the data at 25 and 100 °C have been offset slightly for clarity and do not represent their true positions on the deformation plot.

Not only does adequate spread exist to define deformation paths for individual specimens but, perhaps even more important, sufficient overlap exists between individual paths (20 and 30 %, 30 and 40 %, etc.) that a collective path can be defined for a much larger range of deformations. This appears to be true even though much of the deformation is concentrated within shear zones at the highest total bulk strains, rather than being uniformly distributed throughout the rock. It should be noted, further, that the central mean (indicated by the solid symbol) of each population (i.e. for an individual specimen) represents quite accurately, for strains up to about 40 %, the total bulk strain to which the specimen has been subjected, depending upon the temperature. (As previously mentioned, about 5 % bulk strain is accounted for by the application of hydrostatic pressure.) The central means for the 50 % specimens fall short of the corrected bulk strain by about 7 %, presumably because of the concentrated deformation in shear zones or ductile faults at these high strains.

Conclusions

The results of this study appear to support the following conclusions:

1. Calcitic rocks with uncomplicated burial histories, and especially with high porosity, may have imperceptible yield stresses and may deform continuously under applied differential stress even at relatively fast strain rates.
2. Plane strain may be a typical manner of deformation in limestones naturally deformed to strains of 50 % or less.
3. Limestones deformed at higher temperatures may sustain greater differential stress than those deformed at lower temperatures if the deformation is related to the development of shear zones,
4. Higher temperatures promote greater homogeneity of deformation in limestone and retard the development of shear zones.
5. Higher temperatures promote decreasing width of shear zones.
6. Higher confining pressure inhibits cataclasis, enhances intracrystalline gliding, and promotes greater homogeneity of deformation in limestone.
7. Depending upon the boundary conditions, large strains tend to enhance cataclastic deformation.
8. Certain component strain distributions in deformed rock are effective as a precursor for the development of shear zones.
9. Both individual and collective deformation paths can be derived from component strains in limestones deformed under a range of temperatures and pressures representative of conditions existing at depths in the Earth up to 8 km.

It appears that, although the homogeneity of strain increases with higher confining pressure and higher temperatures, sufficient strain heterogeneity exists among components of the deformed rock that a deformation path can be defined. Moreover, the marked non-homogeneous deformation created by faulting and the development of shear zones does not appear to prevent determination of the deformation path.

PHILOSOPHICAL TRANSACTIONS OF THE ROYAL SOCIETY A MATHEMATICAL, PHYSICAL & ENGINEERING SCIENCES

References (Donath & Wood)

Donath, F. A. 1970 *Am. Scient.* **58**, 54–72.
Donath, F. A., Faill, R. T. & Tobin, D. G. 1971 *Bull. geol. Soc. Am.* **82**, 1441–1462.
Donath, F. A. & Fruth, L. S. 1971 *J. Geol.* **79**, 347–371.
Flinn, D. 1956 *J. Geol.* **64**, 480–505.
Flinn, D. 1962 *Q. J. geol. Soc. Lond.* **118**, 385–433.
Friedman, M. 1963 *J. Geol.* **71**, 12–37.
Handin, J. & Hager, R. V. 1958 *Bull. Am. Ass. Petrol. Geol.* **42**, 2892–2934.
Olsson, W. A. 1974 *Tectonophysics* **24**, 277–285.
Ramsay, J. G. 1967 *Folding and fracturing of rocks*. New York: McGraw-Hill.
Wood, D. S. 1974 *A. Rev. Earth & Planetary Sci.* **2**, 369–401.

PHILOSOPHICAL TRANSACTIONS OF THE ROYAL SOCIETY A MATHEMATICAL, PHYSICAL & ENGINEERING SCIENCES

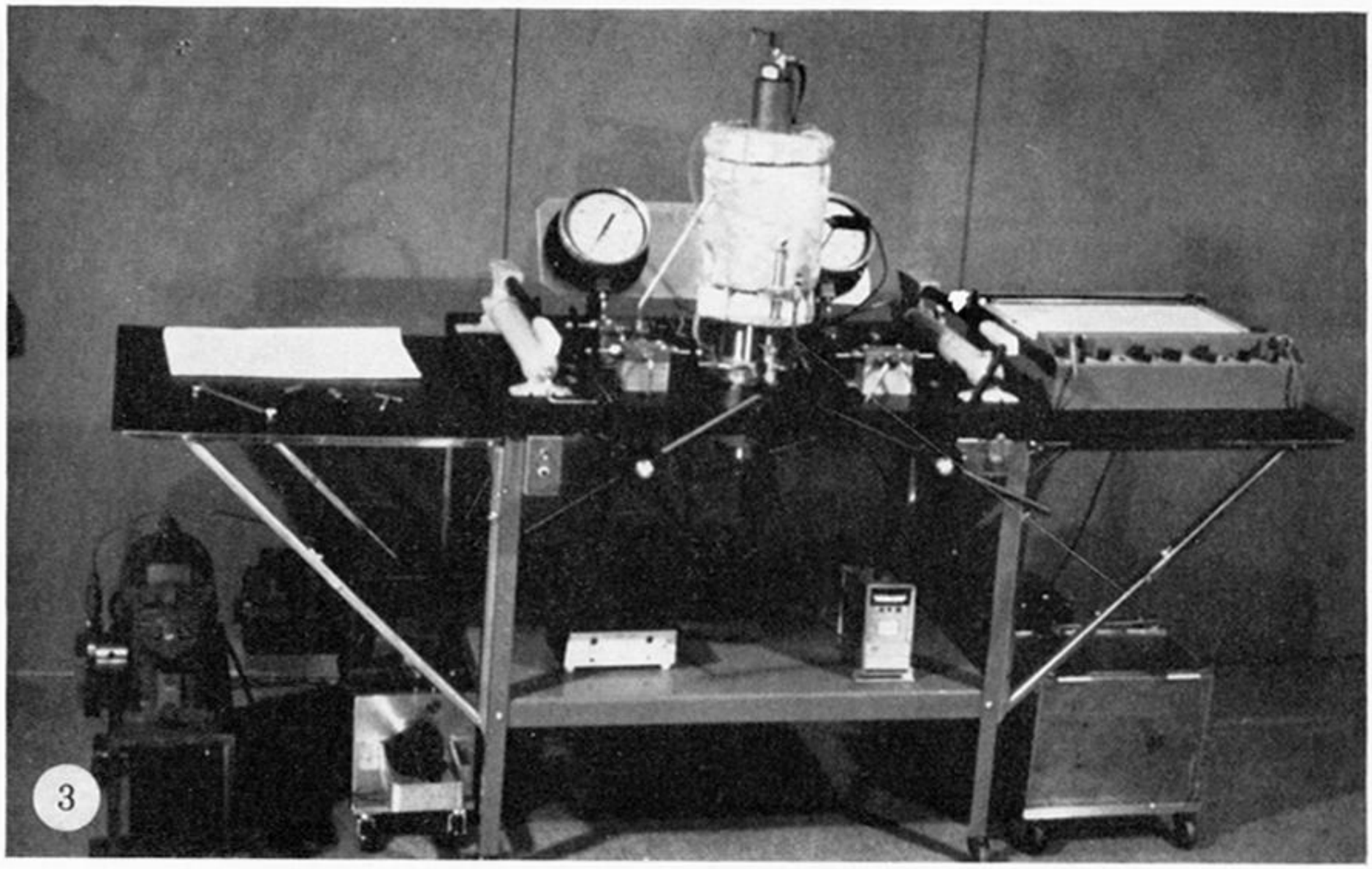

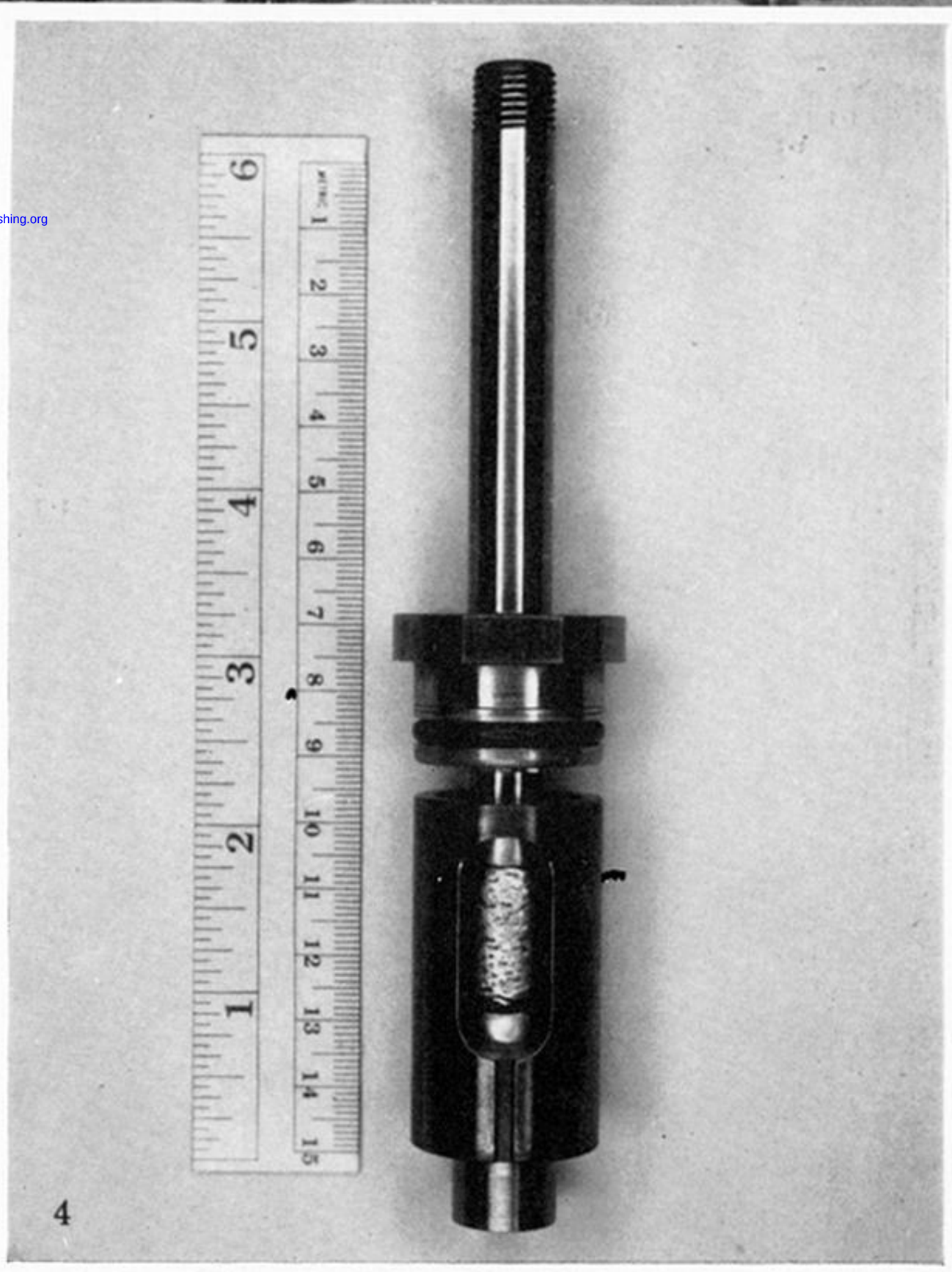

FIGURE 3. Triaxial deformation apparatus. Pressure vessel is shown with heating jacket in place for high temperature experiment. Axial loading pump is positioned beneath bench extension.

FIGURE 4. Constrictor used to effect plane strain condition. Piston-specimen-anvil assembly is shown positioned within constrictor. Specimen has been subjected to 30 % shortening.

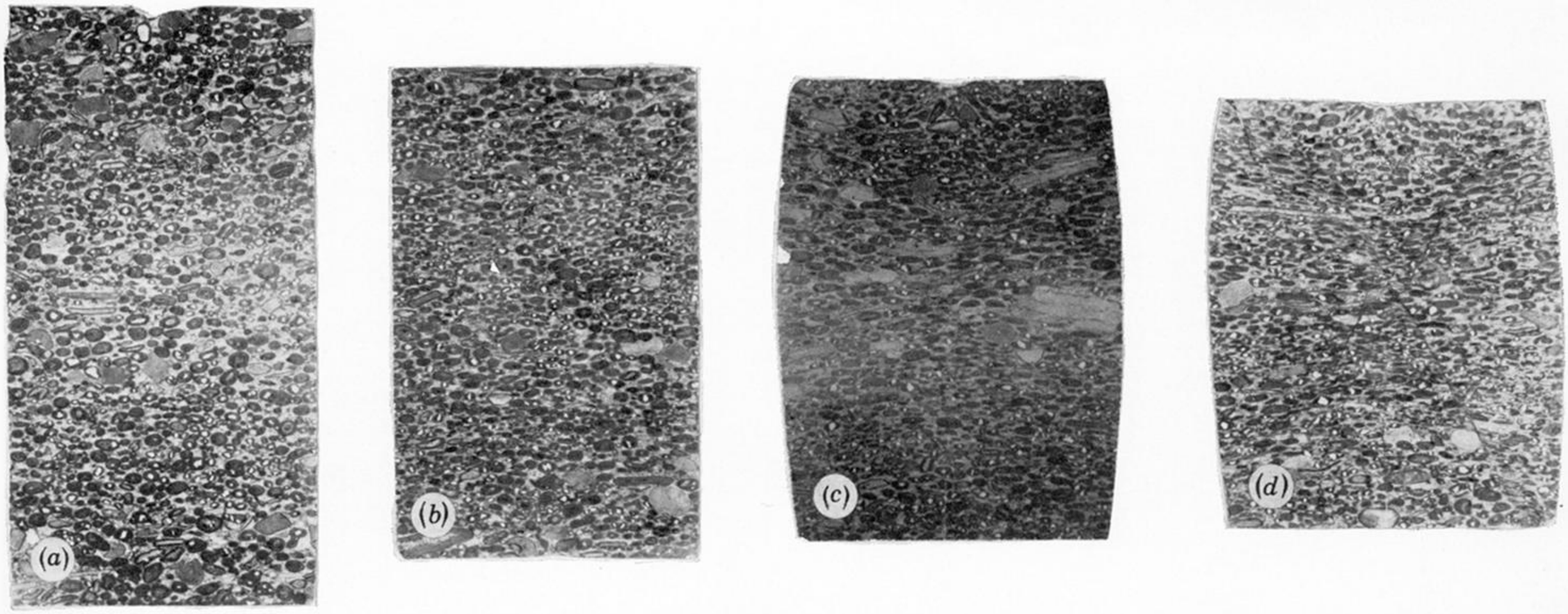

PHILOSOPHICAL TRANSACTIONS OF THE ROYAL SOCIETY A MATHEMATICAL, PHYSICAL & ENGINEERING SCIENCES

FIGURE 9. Photomicrographs of deformed specimens of Inferior oolite. Top row: 200 MPa, 200 °C: *a*, 20 %, *b*, 30 %; *c*, 40 %; *d*, 45 % strain. Middle row: 100 MPa, 200 °C: *n*, 20 %; *o*, 30 %; *p*, 40 %; *q*, 50 % strain. Bottom row: 200 MPa, 25 °C: *j*, 20 %; *k*, 30 %; *l*, 40 %; *m*, 50 % strain.

< 10% 10-15% 15-20% 20-25% 25-30% 30-35% 35-40% 40-45% > 45%

FIGURE 10. For description see opposite.